Impact of carrier frequency offsets on Block-IFDMA systems

E.P. Simon, Virginie Degardin, M. Lienard

Hindawi Publishing Corporation
EURASIP Journal on Wireless Communications and Networking
Volume 2009, Article ID 483128, 7 pages
doi:10.1155/2009/483128

Research Article

Impact of Carrier Frequency Offsets on Block-IFDMA Systems

E. P. Simon, V. Dégardin, and M. Liénard

Telecommunications, Interferences and Electromagnetic Compatibility (TELICE), Institute of Electronics, Microelectronics and Nanotechnology (IEMN) Laboratory, University of Lille, IEMN/UMR 8520, 59655 Villeneuve d_Ascq, France

Correspondence should be addressed to E. P. Simon, eric.simon@univ-lille1.fr

Received 25 June 2008; Accepted 15 December 2008

Recommended by Heidi Steendam

Recently, a new multiple access (MA) scheme called block-interleaved frequency division multiple access (B-IFDMA) is under consideration as an MA scheme candidate for 4G wireless applications. In this paper, the two variants of B-IFDMA are considered, the joint- DFT B-IFDMA and the added-signal B-IFDMA, and compared in terms of sensitivity to carrier frequency offsets (CFOs) for both uplink and downlink. CFO gives rise to multiuser interference and self-user interference. We derive analytical expressions for the power of these interferences, and we quantify their detrimental effect through the evaluation of the signal-to-interference-plus-noise ratio (SINR) degradation. We point out that both variants of B-IFDMA are not similarly affected by CFO. Hence, joint-DFT B-IFDMA provides a better robustness to multiuser interference than added-signal B-IFDMA, and so is better suited for the uplink. Then we show by means of numerical results that added-signal B-IFDMA is less sensitive to CFO in the downlink.

1. Introduction

In the context of the research on beyond 3rd and 4th generation (B3G/4G) mobile radio systems, a novel power-efficient multiple access scheme called block-interleaved frequency multiple access (B-IFDMA) has been proposed as a candidate for nonfrequency-adaptive transmission mode. B-IFDMA is a particular case of discrete Fourier transform (DFT) precoded OFDMA, where the data of the user under consideration is transmitted on blocks of subcarriers that are equidistantly distributed over the total available bandwidth. Hence, it can be viewed as a generalization of DFT precoded OFDMA with interleaved subcarrier allocation, also called IFDMA [1]. Two different variants of B-IFDMA are currently under investigation, the joint-DFT B-IFDMA and the added-signal B-IFDMA [2, 3]. The joint-DFT B-IFDMA signal is based on applying DFT once to all subcarriers assigned to a given user whereas the added-signal B-IFDMA is constructed by applying DFT to groups of subcarriers.

The robustness of B-IFDMA compared to IFDMA to carrier frequency offsets (CFOs) has been discussed in [2] for the uplink. The authors showed that B-IFDMA is expected to be more robust to CFO than IFDMA due to the fact that schemes with interleaved subcarrier allocation are known to be more sensitive to CFO compared to schemes with block allocation. However, it is not clear which variant of B-IFDMA is more robust to CFO. Moreover, to the best of our knowledge, no detailed analysis exists on the sensitivity of B-IFDMA to CFO. The purpose of this paper is to present a comprehensive study of the sensitivity of the joint-DFT and added-signal B-IFDMA to CFO and to compare those two variants in terms of CFO sensitivity.

The effect of CFO on multicarrier schemes has been studied in [4] for OFDM, in [5] for MC-DS-CDMA, and in [6] for MC-CDMA. It was shown that CFO gives rise to signal distortions, yielding interference and power loss which degrades system performance. When this degradation can no longer be tolerated, carrier frequency correction must be applied. For downlink, the CFO is the same for all users. Hence, the carrier frequency can be corrected by using feedback carrier synchronization mechanisms, at the expense of phase jitter [7, 8]. Note that for uplink, since the CFOs associated with different users are different to each other, it is much more difficult to carry out an offset correction [9, 10]. In this paper, we consider both uplink and downlink.

To quantify the performance degradation, we propose to compute the expressions of the signal-to-interference-plus-noise ratio (SINR) degradation for both variants of B-IFDMA. We also provide a detailed analysis of the obtained analytical expressions in order to compare the sensitivity of

both variants to CFO. In addition, numerical results illustrate the analysis.

The paper is organized as follows. In Section 2, a system model including the CFO for both variants of B-IFDMA is given. The sensitivity to CFO is investigated in Section 3. Numerical results are presented in Section 4. Section 5 concludes the paper.

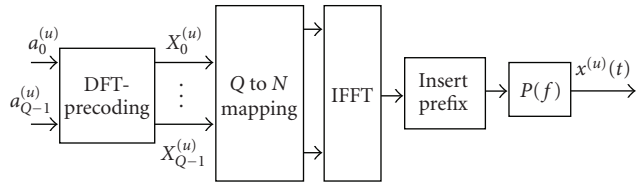

Figure 1: Joint-DFT B-IFDMA transmitter for user u.

2. System Model

In this section, a system model including the CFO is given. As added-signal B-IFDMA model can be generated from IFDMA signals [2], here we focus on the joint-DFT B-IFDMA model. The signal model for IFDMA is described in detail in [11]. The model for joint-DFT B-IFDMA is derived as a particular case of general precoded OFDMA system. Although new algorithms for a lower complexity implementation of B-IFDMA based on time-domain signal generation have been proposed in [3], it is more convenient to perform algebra with the general OFDMA transmitter model.

The joint-DFT B-IFDMA transmitter of user u (see Figure 1) performs a block transmission of Q symbols $a_q^{(u)}$, $q = 0,\ldots,Q-1$, which are assumed to be uncorrelated symbols with power $E_s^{(u)}$.

The first operation consists in a DFT-precoding of the data symbol vector:

$$X_q^{(u)} = \frac{1}{\sqrt{Q}} \sum_{n=0}^{Q-1} a_n^{(u)} c_n^q, \quad q = 0,\ldots,Q-1, \tag{1}$$

where $c_n^q = e^{-j2\pi(nq/Q)}$, $n = 0,\ldots,Q-1$ is a Fourier sequence. Let $N = KQ$ designate the total number of subcarriers available in the OFDMA system, where K is the maximum number of users. Note that N_u will designate the number of active users. Then, the Q precoded symbols $X_q^{(u)}$, $q = 0,\ldots,Q-1$ of user u are transmitted on blocks of subcarriers that are equidistantly distributed over the N subcarriers. Thus, $Q = ML$, where L stands for the number of blocks and M the number of subcarriers per block. The qth symbol $X_q^{(u)}$ modulates the subcarrier of index $M_q^u = lKM+m+uM-N/2$, where $q = lM+m$; $l = 0,\ldots,L-1$; $m = 0,\ldots,M-1$. This mapping is specific to the joint-DFT B-IFDMA scheme.

The N samples of the transmitted sequence are generated by feeding the mapped symbols to an inverse fast Fourier transform. Then, a cyclic prefix of N_g samples is inserted in order to avoid interference caused by dispersive channel. The transmitter feeds those samples at a rate $1/T$ to a unit energy zero roll-off square root Nyquist filter $P(f)$ with respect to the sampling time T.

This results in the continuous- time signal:

$$x^{(u)}(t) = \frac{1}{\sqrt{N}} \sum_{n=-N_g}^{N-1} \sum_{q=0}^{Q-1} X_q^{(u)} \cdot e^{j2\pi(M_q^u n/N)} p(t-nT). \tag{2}$$

The signal $x^{(u)}(t)$ is then transmitted over the dispersive channel from the transmitter of user u to the base station with the channel transfer function $H_{ch}^{(u)}(f)$. The output of the dispersive channel is disturbed by a carrier phase error which linearly increases in time within an OFDM symbol period: $\Phi^{(u)}(t) = 2\pi\Delta F^{(u)}t + \Phi^{(u)}(0)$, where $\Delta F^{(u)}$ stands for the CFO for user u. Without loss of generality, we assume $\Phi^{(u)}(0) = 0$. We also assume small CFO compared to the bandwidth of the receiver filter $\Delta F^{(u)}T \ll 1$.

The base station receives the sum of the signals transmitted by the different users, disturbed by additive white Gaussian noise $w(t)$, with uncorrelated real and imaginary parts, each having a power spectral density N_0. The resulting signal enters the receiver filter, which is matched to the transmitted filter and is sampled at instants $t_k = kT$ assuming perfect timing synchronization.

Without loss of generality, we focus on the detection of the data symbols transmitted by the user u. Moreover, to clearly emphasize the effect of CFO, a transmission over a nondispersive channel for each user is considered from now on, that is, $H_{ch}^{(u)}(f) = 1$, $u = 0,\ldots,N_u-1$. So, in order to detect the data symbols of user u, the samples corresponding to the cyclic prefix are removed and the remaining N samples are fed to the discrete Fourier transform. Note that an equalizer should be used to compensate for the systematic phase rotation of the FFT outputs. However, the equalizer is not able to eliminate interference caused by CFO. As the topic of this paper is to study the effect of CFO, it is not useful to include the equalizer in the analysis. Then, Q samples are taken from the N resulting frequency domain samples according to the specific mapping of user u. Those Q samples are de-precoded by means of an inverse DFT operation. The qth resulting sample, denoted $z_q^{(u)}$, is used to make a decision about the data symbol $a_q^{(u)}$. The sample $z_q^{(u)}$ can be written

$$z_q^{(u)} = \sum_{u'=0}^{N_u-1} \sum_{q'=0}^{Q-1} a_{q'}^{(u')} I_{q,q'}^{u,u'} + W_q^{(u)}, \tag{3}$$

where $W_q^{(u)}$ is a white complex Gaussian noise with variance $2N_0$ and $I_{q,q'}^{u,u'}$ is the contribution of the symbol $a_{q'}^{(u')}$ to the input of the decision device. The next paragraph deals with the computation of the quantity $I_{q,q'}^{u,u'}$.

Let us now define an equivalent time-varying channel for a given user u including the carrier phase errors and the transmitter and receiver filters. As $\Delta F^{(u)}$ is much smaller than $1/T$, the variation of the phase error over the impulse response duration of the receiver filter can be safely neglected. Its Fourier transform is then given by

$$H_{eq}^{(u)}(f;t_k) = |P(f)|^2 e^{j\Phi^{(u)}(t_k)}. \tag{4}$$

Assuming a sufficient cyclic prefix length, $I_{q,q'}^{u,u'}$ finally reduces to

$$I_{q,q'}^{u,u'} = \frac{1}{Q}\sum_{p=0}^{Q-1}\sum_{p'=0}^{Q-1} c_p^{q^*} c_{p'}^{q'} \frac{1}{N}\sum_{k=0}^{N-1} e^{j2\pi k(M_{p'}^{u'}-M_p^u)/N} G_{M_{p'}^{u'}}^{(u')}(t_k), \quad (5)$$

where

$$G_n^{(u')}(t_k) = \frac{1}{T}\sum_{m=-\infty}^{+\infty} H_{eq}^{(u')}\left(\frac{n}{NT}+\frac{m}{T};t_k\right) \quad (6)$$

is the folded transfer function of the equivalent channel defined in (4) evaluated at the frequencies n/NT.

The quantities $I_{q,q'}^{u,u'}$, $q' = 0,\ldots,Q-1$, $u' = 0,\ldots,N_u-1$ can be classified into several contributions. The first contribution obtained for $q' = q$, $u' = u$ is the useful contribution. It can be decomposed into an average useful component $E\{I_{q,q}^{u,u}\}$ and a zero-mean fluctuation $I_{q,q}^{u,u} - E\{I_{q,q}^{u,u}\}$ around its average, called self-interference. The contribution obtained for $(q' \neq q,\ u' = u)$ is the intrablock interference, caused by the other symbols transmitted by the desired user u. From now on, we group the self-interference and the intrablock interference both caused by the desired user in order to only consider one interference term called the self-user interference (SUI). The last contribution $(u' \neq u)$ is the multiuser interference (MUI). To measure the performance of the system, we use the SINR which is the ratio of the power of the average useful component to the sum of the power of the additive noise with the interference. When CFOs are present, the SINR is degraded compared to the case with no synchronization errors. Then, we compute the SINR degradation caused by CFO. The SINR is defined as

$$\mathrm{SINR}_q^{(u)} = \frac{E_s^{(u)} P_{U,q}^{(u)}}{2N_0 + E_s^{(u)}\left(P_{\mathrm{SUI},q}^{(u)} + P_{\mathrm{MUI},q}^{(u)}\right)}, \quad (7)$$

where

$$P_{U,q}^{(u)} = \left|E\{I_{q,q}^{u,u}\}\right|^2, \quad (8)$$

$$P_{\mathrm{SUI},q}^{(u)} = E\left\{\left|I_{q,q}^{u,u} - E\{I_{q,q}^{u,u}\}\right|^2\right\} + \sum_{q'=0;\,q'\neq q}^{Q-1} E\left\{\left|I_{q,q'}^{u,u}\right|^2\right\}, \quad (9)$$

$$P_{\mathrm{MUI},q}^{(u)} = \sum_{u'=0;\,u'\neq u}^{N_u-1}\sum_{q'=0}^{Q-1} \frac{E_s^{(u')}}{E_s^{(u)}} E\left\{\left|I_{q,q'}^{u,u'}\right|^2\right\}. \quad (10)$$

In the absence of synchronization errors, the SINR becomes independent of the symbol index q and is given by

$$\mathrm{SINR}^{(u)}(0) = \frac{E_s^{(u)}}{2N_0}, \quad (11)$$

whereas in the presence of synchronization errors, the SINR is reduced compared to $\mathrm{SINR}^{(u)}(0)$. The degradation of the SINR compared to $\mathrm{SINR}^{(u)}(0)$ expressed in decibels is finally given by

$$\mathrm{Deg} = -10\log\left(\frac{P_{U,q}^{(u)}}{1+\mathrm{SINR}^{(u)}(0)\left(P_{\mathrm{SUI},q}^{(u)}+P_{\mathrm{MUI},q}^{(u)}\right)}\right). \quad (12)$$

3. Impact of Carrier Frequency Offset on B-IFDMA

In this section, we investigate the effect of CFO to the performance of the two B-IFDMA variants, the joint-DFT B-IFDMA and the added-signal B-IFDMA. First, we consider the joint-DFT B-IFDMA signal.

3.1. Joint-DFT B-IFDMA. Under the assumption of a nondispersive channel, (6) becomes

$$G_n^{(u')}(kT) = e^{j2\pi\Delta F^{(u')}kT}. \quad (13)$$

Thus, (5) reduces to

$$I_{q,q'}^{u,u'} = \frac{1}{Q}\sum_{p=0}^{Q-1}\sum_{p'=0}^{Q-1} c_p^{q^*} c_{p'}^{q'} D_N\left(\frac{M_{p'}^{(u')}-M_p^{(u)}}{N}+\Delta F^{(u')}T\right), \quad (14)$$

where $D_N(x)$ is defined as

$$D_N(x) = \frac{1}{N}\sum_{n=0}^{N-1} e^{2j\pi nx} = e^{j\pi(N-1)x}\frac{\sin\pi Nx}{N\sin\pi x}. \quad (15)$$

The power of the average useful component, the self-user interference and the multiuser interference are computed by inserting (14) in (8), (9), and (10), respectively. The details of the computation are reported in the appendix, yielding (16), (17), and (18):

$$P_U^{(u)} = \left|D_N\left(\Delta F^{(u)}T\right)\right|^2, \quad (16)$$

$$P_{\mathrm{SUI}}^{(u)} = A^{(u,u)}\left(\Delta F^{(u)}\right) - \left|D_N\left(\Delta F^{(u)}T\right)\right|^2, \quad (17)$$

$$P_{\mathrm{MUI}}^{(u)} = \sum_{u'=0;\,u'\neq u}^{N_u-1}\frac{E_s^{(u')}}{E_s^{(u)}} \times \left(A^{(u,u')}\left(\Delta F^{(u')}\right) - \left|D_N\left(\frac{(u'-u)M}{N}+\Delta F^{(u')}T\right)\right|^2\right). \quad (18)$$

Note that since the obtained expressions are independant of the desired symbol index q, we have dropped this index. In (17) and (18), the term $A^{(u,u')}(\Delta F^{(u')})$ is defined in (19):

$$A^{(u,u')}(f) = \frac{1}{M}\sum_{m=-(M-1)}^{M-1}(M-|m|) \times \left|D_{KM}\left(L\left(fT+\frac{(u'-u)M+m}{N}\right)\right)\right|^2. \quad (19)$$

Note that since $D_N(x)$ is periodic of period 1, $A^{(u,u')}(f)$ is a periodic function with period $1/LT = KM/NT$, which corresponds to the spacing between two blocks of M adjacent subcarriers. Also note that when M increases, it can be

shown that the pattern of the periodic function tends to the following triangular function:

$$\Lambda(f) = \begin{cases} 1 - \left| f\dfrac{NT}{M} \right|, & |f| < \dfrac{M}{NT}, \\ 0, & \text{otherwise.} \end{cases} \tag{20}$$

Figure 2 shows the plots of $A^{(u,u)}(f)$ and $D_N(f)$ for $M = 8$, $L = 2$, and $K = 2$.

In addition to the interference terms, it follows from (16) that the useful component at the FFT output is reduced compared to the case of a zero CFO. Hence, to keep the power loss within reasonable bounds, the CFO must satisfy $\Delta F^{(u)}T \ll 1/N$ which is easy to understand since the IFFT behaves like a bank of filters of bandwidth $1/(NT)$.

The resulting expression of the degradation for joint-DFT B-IFDMA is obtained by inserting (16), (17), and (18) in (12).

3.2. Added-Signal B-IFDMA. The added-signal B-IFDMA model for a given user comes from the superimposing of M IFDMA signals, each with L subcarriers [2]. These M IFDMA signals are mutually shifted by one subcarrier bandwidth.

On the other hand, the signal model for IFDMA can be viewed as a particular case of joint-DFT B-IFDMA, where the block size M equals 1. Hence, from these two remarks and from the results obtained in Section 3.1, it is straightforward to compute the interference power expressions for the added-signal B-IFDMA. The useful power is the same as that of joint-DFT B-IFDMA, given by (16). The interference power expressions are given by (21) and (22):

$$P_{\text{SUI}}^{(u)} = \sum_{m=0}^{M-1} \left(\left| D_{KM}\left(L\left(\Delta F^{(u)}T + \frac{m}{N} \right) \right) \right|^2 - \left| D_N\left(\Delta F^{(u)}T + \frac{m}{N} \right) \right|^2 \right), \tag{21}$$

$$P_{\text{MUI}}^{(u)} = \sum_{u'=0;\, u' \neq u}^{N_u - 1} \frac{E_s^{(u')}}{E_s^{(u)}} \times \sum_{m=0}^{M-1} \left(\left| D_{KM}\left(L\left(\Delta F^{(u')}T + \frac{m + (u'-u)M}{N} \right) \right) \right|^2 - \left| D_N\left(\Delta F^{(u')}T + \frac{m + (u'-u)M}{N} \right) \right|^2 \right). \tag{22}$$

The resulting expression of the degradation for added-signal B-IFDMA is obtained by inserting (16), (21), and (22) in (12).

3.3. Comparison of Sensitivity to CFO for Both Variants of B-IFDMA. To compare both variants of B-IFDMA in terms of sensitivity to CFO, we analyze the interference power expressions obtained in the previous sections. We start with the analysis of the SUI power. From (17) and from the shape of the functions $A^{(u,u)}(f)$ and $D_N(fT)$ given in Figure 2, it follows that to obtain small SUI power for joint-DFT B-IFDMA, $\Delta F^{(u)}T$ must be limited, that is, $\Delta F^{(u)}T \ll 1/N$. On the contrary, it follows from (21) that the SUI power for added-signal B-IFDMA is very small even for $\Delta F^{(u)}T > 1/N$. Figure 3 illustrates the SUI power as a function of $\Delta F^{(u)}$ for $M = 8$, $L = 2$, and $K = 2$. Let us now consider the MUI power. Note that for both variants of B-IFDMA, the interference power due to user u', $u' \neq u$, can be obtained by shifting in frequency domain the SUI power expression by $(u' - u)M/NT$ and by evaluating it at the frequency $\Delta F^{(u')}$. Hence, when considering the joint-DFT B-IFDMA, even when the condition $\Delta F^{(u)}T \ll 1/N$ is not satisfied, the MUI power value is small which is not the case for added-signal B-IFDMA (see Figure 3).

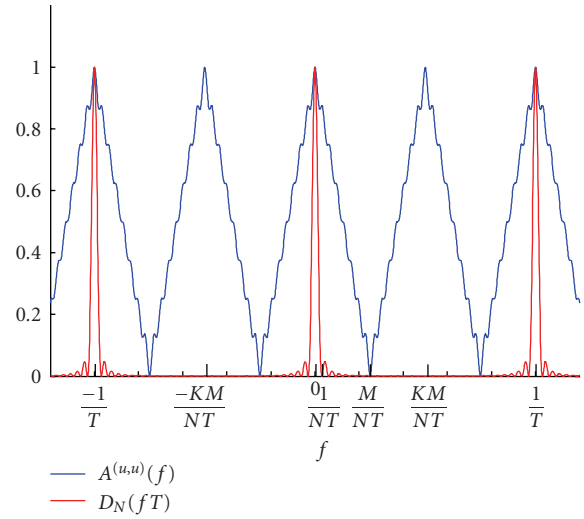

Figure 2: Plot of $A^{(u,u)}(f)$ and $D_N(fT)$ for $M = 8$, $L = 2$, and $K = 2$.

In summary, it turns out that for the joint-DFT B-IFDMA, most of the interference comes from the SUI whereas the added-signal B-IFDMA mostly suffers from the MUI. Numerical results are presented in Section 4 to illustrate this analysis.

4. Numerical Results

In this section, we present numerical results of SINR degradations due to CFO for the joint-DFT B-IFDMA and added-signal B-IFDMA. We assume the same CFO ΔF for all users, that is, $\Delta F^{(u')} = \Delta F$ for $u' = 0, \ldots, K-1$. We also assume that all users exhibit the same energy per symbol with $Q = 64$ subcarriers assigned to each user. The maximum number of users is $K = 8$ and $\text{SINR}(0) = 25$ dB.

Figure 4 shows the SINR degradation computed with (12) as a function of ΔF for the full load with $M = 8$ subcarriers per block and $L = 8$ blocks. As expected, we observe that both variants are very sensitive to CFO. Hence, in order to keep the degradation value small (say, less than 0.5 dB), it is required that $\Delta F < 0.01/NT$.

We also observe that the joint-DFT B-IFDMA is less robust to CFO than added-signal B-IFDMA. For instance,

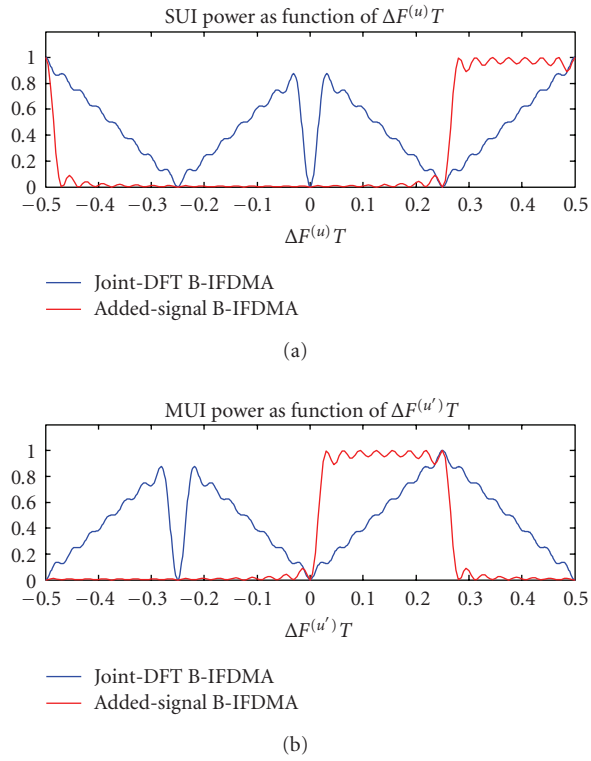

FIGURE 3: SUI power and MUI power for $M = 8$, $L = 2$ and $K = 2$.

for the same CFO of $0.03/NT$, the degradation with the joint-DFT B-IFDMA is 1 dB higher than that with the added-signal B-IFDMA.

For the sake of comparison, we plot the degradation obtained for IFDMA systems. The considered IFDMA system has the same number of subcarriers assigned to each user ($Q = 64$), which are equidistantly distributed over the total bandwidth [11]. As IFDMA can be regarded as a special case of joint-DFT B-IFDMA with $M = 1$, it is straightforward to obtain the degradation expression.

As we observe, the degradation value for IFDMA is very close to that of the added-signal B-IFDMA. Hence, as the added-signal B-IFDMA model is obtained by superimposing IFDMA signals, the behavior of both systems is nearly similar in terms of CFO sensitivity.

In Figure 5, the degradation value is shown as a function of the number of active users for $\Delta F = 0.02/NT$ with three different sets of values of M and L. First, we consider $M = 8$ and $L = 8$, then $M = 4$ and $L = 16$, and finally $M = 2$ and $L = 32$. As already mentioned earlier, when the load is maximum, the joint-DFT B-IFDMA is more sensitive to CFO than the added-signal B-IFDMA. However, for the joint-DFT B-IFDMA, we observe that the degradation value is near its maximum with just one active user (above all for high values of M). This means that the degradation is essentially dominated by the SUI and that contribution of the MUI is weak. On the contrary, the MUI contribution is the dominant one for the added-signal B-IFDMA. Hence, the joint-DFT B-IFDMA is better suited than the added-signal B-IFDMA in terms of CFO sensitivity if an uplink

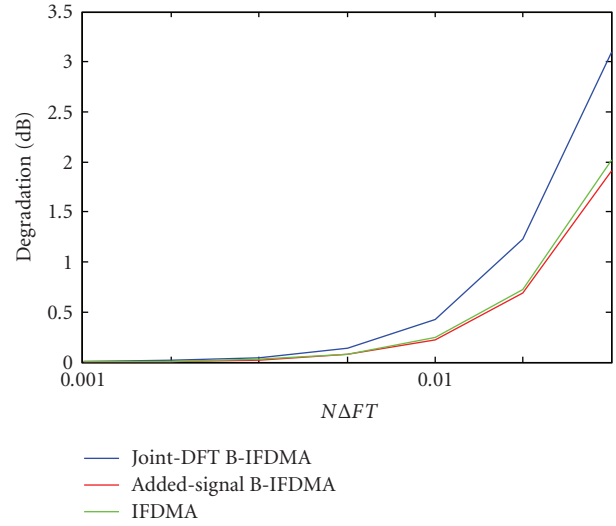

FIGURE 4: Degradation as a function of ΔF for the full load with $M = 8$, $L = 8$ (yielding $Q = 64$), and $K = 8$.

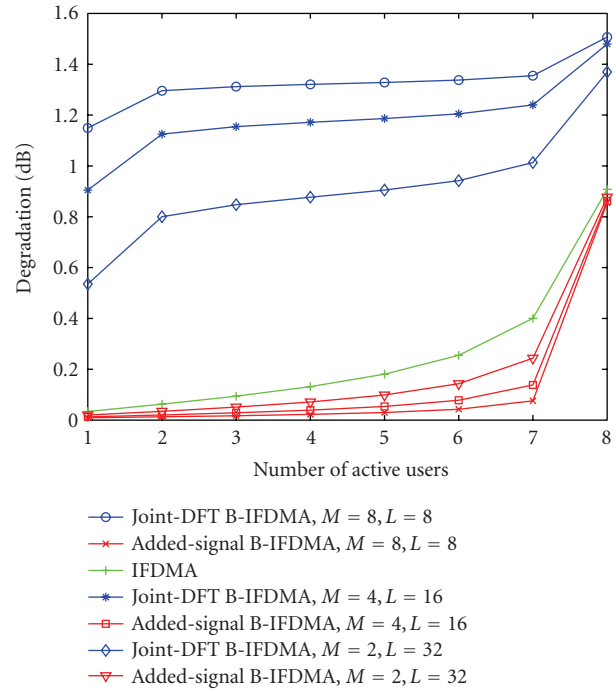

FIGURE 5: Degradation as a function of number of active users with $\Delta F = 0.02/NT$, $Q = 64$, and $K = 8$.

is considered. On the other hand, for the downlink, it has been shown that the added-signal B-IFDMA is more robust to CFO than the joint-DFT B-IFDMA. Note that this general trend may no longer be valid if the number of subcarriers per block M is small. Indeed, when M decreases, B-IFDMA signal model tends toward IFDMA signal model, and for the particular case of $M = 1$, B-IFDMA corresponds to IFDMA. This is observed in Figure 5 wherein the behavior for both variants of B-IFDMA tends toward that of IFDMA when M is decreased.

5. Conclusion

In this paper, the two variants of B-IFDMA, the joint-DFT B-IFDMA and the added-signal B-IFDMA, have been investigated in terms of carrier frequency offset (CFO) sensitivity. CFO gives rise to useful power loss together with interference, leading to performance degradation. To evaluate this performance degradation, we have determined the theoretical expressions of the SINR degradation caused by CFO at the input of the decision device. The results of the analysis have shown a different behavior for both variants of B-IFDMA in terms of CFO sensitivity. Hence, when considering the added-signal B-IFDMA, the multiuser interference contributions are the dominant ones. For the joint-DFT B-IFDMA, the degradation is found to be dominated by self-user interference. As a consequence, it appears that, in terms of sensitivity to CFO, joint-DFT B-IFDMA is better suited than added-signal B-IFDMA for the uplink. Indeed, the effect of multiuser interference is far more complex to be corrected with the uplink case than downlink. Then, the numerical results have shown that the added-signal B-IFDMA is more robust to CFO for the downlink.

Appendix

The purpose of this appendix is to give an outline of the main steps leading to the evaluation of the interference power caused by CFO for the joint-DFT B-IFDMA. A simple way to perform computations of the useful and interference power expressions is to follow an approach similar to the approach used for MC-CDMA with orthogonal spreading sequences (Walsh-Hadamard) [7, 12]. Let Q be the spreading factor. In this approach, although the used spreading sequences contain no randomness, the authors introduce randomness by assuming that each of the Q sequences can be assigned with a probability $1/Q$ to the first user, each of the remaining $(Q-1)$ sequences can be assigned with a probability $1/(Q-1)$, and so on. Thus, we obtain averages over all users of the expressions for nonrandom Walsh-Hadamard sequences. On the other hand, as IFDMA can be viewed as a fully loaded spread spectrum multicarrier transmission scheme [11], where the spreading sequences are Fourier sequences, and since the Fourier sequences are also orthogonal, we can safely extend this approach to the B-IFDMA. This approach leads to using the following formulas [7]:

$$E\{c_n^{q*} c_{n'}^{q}\} = \delta_{n,n'}, \tag{A.1}$$

where $\delta_{n,n'}$ equals 1 if $n = n'$ and 0 otherwise.

$$E\{c_n^{q*} c_{n'}^{q} c_m^{q*} c_{m'}^{q}\} = \delta_{n,m}\delta_{n',m'} + \delta_{n,n'}\delta_{m,m'} - \delta_{n,n',m,m'} \tag{A.2}$$

where $\delta_{n,n',m,m'} = \delta_{n,n'}\delta_{m,m'}\delta_{n,m}$,

$$E\{c_n^{q*} c_{n'}^{q'} c_m^{q*} c_{m'}^{q'}\} = \delta_{n,m}\delta_{n',m'} - \frac{1}{Q-1}\left(\delta_{n,n'}\delta_{m,m'} - \delta_{n,n',m,m'}\right). \tag{A.3}$$

To begin with, let us focus on the useful power expression. We first use (14) in (8). Then, by using (A.1), it is straightforward to find (16). The computation of the interference power needs more stages. Let us consider the self-interference (SI) power computation. Using (14) in the first term of (9) yields a first expression. Then, using (A.2) in this expression yields after some computations (A.4):

$$P_{\mathrm{SI}}^{(u)} = \frac{1}{Q^2}\sum_{p=0}^{Q-1}\sum_{p'=0}^{Q-1}\left|D_N\left(\frac{M_{p'}^{(u)} - M_p^{(u)}}{N} + \Delta F^{(u)}T\right)\right|^2 - \frac{1}{Q}\left|D_N\left(\Delta F^{(u)}T\right)\right|^2. \tag{A.4}$$

We do the same for the intrablock interference (IBI), (resp., MUI) by using (A.2) (resp., (A.3)), yielding (A.5) and (A.6):

$$P_{\mathrm{IBI}}^{(u)} = \frac{Q-1}{Q^2}\sum_{p=0}^{Q-1}\sum_{p'=0}^{Q-1}\left|D_N\left(\frac{M_{p'}^{(u)} - M_p^{(u)}}{N} + \Delta F^{(u)}T\right)\right|^2 - \frac{Q-1}{Q}\left|D_N\left(\Delta F^{(u)}T\right)\right|^2, \tag{A.5}$$

$$P_{\mathrm{MUI}}^{(u)} = \sum_{u'=0;u'\neq u}^{N_u-1}\frac{E_s^{(u')}}{E_s^{(u)}} \times\left(\frac{1}{Q}\sum_{p=0}^{Q-1}\sum_{p'=0}^{Q-1}\left|D_N\left(\frac{M_{p'}^{(u')} - M_p^{(u)}}{N} + \Delta F^{(u')}T\right)\right|^2 - \left|D_N\left(\frac{(u'-u)M}{N} + \Delta F^{(u')}T\right)\right|^2\right). \tag{A.6}$$

Let us now put those expressions in a concatenated form in order to facilitate their interpretation. Define $A^{(u,u')}(\Delta F^{(u')})$ as follows:

$$A^{(u,u')}\left(\Delta F^{(u')}\right) = \frac{1}{Q}\sum_{p=0}^{Q-1}\sum_{p'=0}^{Q-1}\left|D_N\left(\frac{M_{p'}^{(u')} - M_p^{(u)}}{N} + \Delta F^{(u')}T\right)\right|^2. \tag{A.7}$$

We develop $A^{(u,u')}(\Delta F^{(u')})$ by first using the definition of the joint-DFT specific mapping given in Section 2. Hence, the summation over p (resp., p') becomes a summation over l and m (resp., l' and m'), where $p = lM + m$ (resp., $p' = l'M + m'$). Then, the use of (15) in (A.7) yields (A.8) after rearranging the terms:

$$A^{(u,u')}\left(\Delta F^{(u')}\right) = \frac{1}{QN^2}\sum_{n=0}^{N-1}\sum_{n'=0}^{N-1} e^{j2\pi(n-n')\left(\Delta F^{(u')}T + ((u'-u)M/N)\right)} \times\sum_{m=0}^{M-1}\sum_{m'=0}^{M-1} e^{j(2\pi/N)(n-n')(m'-m)} \times\sum_{l'=0}^{L-1} e^{j(2\pi/L)l'(n-n')}\sum_{l=0}^{L-1} e^{-j(2\pi/L)l(n-n')}. \tag{A.8}$$

The last summation in (A.8) reduces to

$$\sum_{l=0}^{L-1} e^{-j(2\pi/L)l(n-n')} = \begin{cases} L, & \text{for } n-n' = \alpha L, \\ 0, & \text{otherwise,} \end{cases} \tag{A.9}$$

where α is an integer. Let us now decompose n ($n = 0,\ldots,N-1$) as $n = \mu L + \lambda$, ($\mu = 0,\ldots,KM-1$, $\lambda = 0,\ldots,L-1$). Similarly, $n' = \mu' L + \lambda'$. From (A.9), it follows that the last summation in (A.8) equals L only for $\lambda = \lambda'$. With this substitution and after some rearrangement, (A.8) becomes

$$A^{(u,u')}\left(\Delta F^{(u')}\right) = \frac{1}{M}\sum_{m=0}^{M-1}\sum_{m'=0}^{M-1} \times \left| D_{KM}\left(L\left(\Delta F^{(u')}T + \frac{(u'-u)M + m' - m}{N}\right)\right)\right|^2. \tag{A.10}$$

Finally, $A^{(u,u')}(\Delta F^{(u')})$ reduces to (19). Thus, we obtain the interference power expressions given in (17) and (18), with $A^{(u,u')}(\Delta F^{(u')})$ defined in (19).

Acknowledgments

This work has been carried out in the framework of the Campus International sur la Sécurité et l Intermodalité des Transports (CISIT) project and funded by the French Ministry of Research, the Region Nord Pas de Calais, and the European Commission (FEDER funds).

References

[1] U. Sorger, I. De Broeck, and M. Schnell, "Interleaved FDMA—a new spread-spectrum multiple-access scheme," in *Proceedings of the IEEE International Conference on Communications (ICC '98)*, vol. 2, pp. 1013–1017, Atlanta, Ga, USA, June 1998.

[2] T. Svensson, T. Franky, D. Falconer, M. Sternad, E. Costa, and A. Klein, "B-IFDMA—a power efficient multiple access scheme for non-frequency-adaptive transmission," in *Proceedings of the 16th IST Mobile and Wireless Communications Summit*, pp. 1–5, Budapest, Austria, July 2007.

[3] T. Frank, A. Klein, and E. Costa, "An efficient implementation for block-IFDMA," in *Proceedings of the 18th IEEE International Symposium on Personal, Indoor and Mobile Radio Communications (PIMRC '07)*, pp. 1–5, Athens, Greece, September 2007.

[4] T. Pollet, M. Van Bladel, and M. Moeneclaey, "BER sensitivity of OFDM systems to carrier frequency offset and Wiener phase noise," *IEEE Transactions on Communications*, vol. 43, no. 2–4, pp. 191–193, 1995.

[5] H. Steendam and M. Moeneclaey, "The effect of carrier frequency offsets on downlink and uplink MC-DS-CDMA," *IEEE Journal on Selected Areas in Communications*, vol. 19, no. 12, pp. 2528–2536, 2001.

[6] H. Steendam and M. Moeneclaey, "The sensitivity of MC-CDMA to synchronisation errors," *European Transactions on Telecommunications*, vol. 10, no. 4, pp. 429–436, 1999.

[7] H. Steendam and M. Moeneclaey, "The effect of carrier phase jitter on MC-CDMA performance," *IEEE Transactions on Communications*, vol. 47, no. 2, pp. 195–198, 1999.

[8] E. Simon, R. Legouable, M. Hélard, and M. Liénard, "Impact of phase and timing jitter on IFDMA systems," *European Transactions on Telecommunications*, vol. 19, no. 6, pp. 697–705, 2008.

[9] J. Choi, C. Lee, H. W. Jung, and Y. H. Lee, "Carrier frequency offset compensation for uplink of OFDM-FDMA systems," *IEEE Communications Letters*, vol. 4, no. 12, pp. 414–416, 2000.

[10] Z. Cao, U. Tureli, and Y.-D. Yao, "Deterministic multiuser carrier-frequency offset estimation for interleaved OFDMA uplink," *IEEE Transactions on Communications*, vol. 52, no. 9, pp. 1585–1594, 2004.

[11] M. Schnell, I. De Broeck, and U. Sorger, "A promising new wideband multiple-access scheme for future mobile communications systems," *European Transactions on Telecommunications*, vol. 10, no. 4, pp. 417–427, 1999.

[12] H. Steendam and M. Moeneclaey, "MC-CDMA performance in the presence of timing errors," in *Proceedings of the 2nd Conference on Telecommunications (ConfTele '99)*, pp. 211–215, Sesimbra, Portugal, April 1999.